Fusion Engineering and Design 157 (2020) 111816

Contents lists available at ScienceDirect

Fusion Engineering and Design

journal homepage: www.elsevier.com/locate/fusengdes

Fast scenario design for alternative magnetic diverted discharge on EAST

Z.P. Luo[a], Y. Huang[a,*], Q.P. Yuan[a], B.J. Xiao[a,b]

[a] Institute of Plasma Physics, Chinese Academy of Sciences, Hefei, 230031, China
[b] School of Nuclear Science and Technology, University of Sciences and Technology, Hefei, 230031, China

ARTICLE INFO

Keywords:
Fast scenario design
Alternative magnetic diverted configuration
Plasma control system
Plasma equilibrium optimization
EAST tokamak

ABSTRACT

In order to develop a new alternative magnetic diverted (AMD) discharge on EAST, it is necessary to define a series of target configuration parameters on plasma control system (PCS), especially this new configuration requires a strong effort on the poloidal field (PF) coil currents. By combining the static equilibrium configuration optimization and flux consuming estimation for PF coils current, multiple basic scenarios with exactly the same target configuration were designed for different stages on plasma current flat-top phase. The high PF coil currents requirement was optimized by the specific equilibrium design procedure to keep them away from the limitation. In this paper, we present the fast scenario design details, together with the experiments results.

1. Introduction

Heat and particle loads on the plasma facing components are one of the most serious challenging to be solved for the future tokamak fusion reactor [1,2]. One approach to handle the heat exhaust is to use alternative magnetic configurations, such as the snowflake divertor [3] and (super-)X-divertor [4,5]. The X-divertor places the second x-point near the plate, causing flared field lines there, which spreads the heat over a large area and increases the line connection length.

As shown in Fig. 1, EAST is constructed to be up-down symmetric, with the following main parameters [6]: major radius $R = 1.8$ m, minor radius $a = 0.45$ m, toroidal field B_T up to 3.5 T, and plasma current I_p up to 1MA for highly elongated plasmas with an elongation $\kappa = 1.9$. It can be operated in quite flexible plasma shapes with an elongation factor $\kappa = 1.5 \sim 2.0$ and triangularity $\delta = 0.3 \sim 0.6$ for double null or single null diverted configurations. EAST equipped with 14 superconducting PF coils for ohmic heating, ohmic current drive, plasma shaping and position control located outside the toroidal field coils [7]. It should be noted that PF7 and PF9 are permanent connected in series, so are PF8 and PF10. For the fast control of the vertical motion of the elongated plasma, a pair of inside coils (IC1 & IC2) in normal state are connected in anti-series and driven by a fast power supply. Exact snowflake for EAST is only possible at very low plasma current due to poloidal coil system limitation. However, an alternative magnetic diverted configuration [8], characterized by two first-order X points where one is located in the primary separatrix and the other is outside the vacuum vessel, can be optimized to satisfy EAST constraints. In order to build these AMD discharges on EAST, a fast scenario design method based on F2EQ [9] code has been developed, the following parts will present the design method and the experiment validation results.

2. Fast scenario design

In order to achieve this AMD configuration, the desired plasma position and shape should be carefully designed to satisfy the EAST tokamak constraints and controlled by the plasma control system. In this fast scenario design method, two prerequisites are defined. First, the target AMD configuration will be optimized for plasma current on flat-top phase. Second, the target plasma shape in all scenarios will be exactly the same, which means the shaping currents component in PF coils will be same in all these scenarios. Since we only focus on the plasma current flat-top phase, the scenarios for plasma breakdown and ramp-up will be inherited from the routine EAST plasma discharges.

For the new AMD configuration, PCS needs a set of plasma parameters to describe its evolution, such as the plasma current I_p, plasma current center coordinates (R_p, Z_p), elongation κ, triangularity δ, internal inductance ι_i, poloidal beta β_p and the PF coil currents. A generally accpeted method for calculating these parameters is to find the PF coil currents according to the given ohmic flux consuming at the variantions of these parameters and plasma shape. Since all the designed scenarios will have same plasma current level and plasma shape, most of these parameters will be optimized for one given target configuration except the PF coil currents. Currents induced in passive structures are neglected, which is reasonable for the unchanged plasma current at flat-top phase.

The ideal design way usually has two steps. First, target plasma

* Corresponding author.
E-mail address: yaohuang@ipp.ac.cn (Y. Huang).

https://doi.org/10.1016/j.fusengdes.2020.111816
Received 10 August 2019; Received in revised form 9 March 2020; Accepted 3 June 2020
Available online 09 June 2020

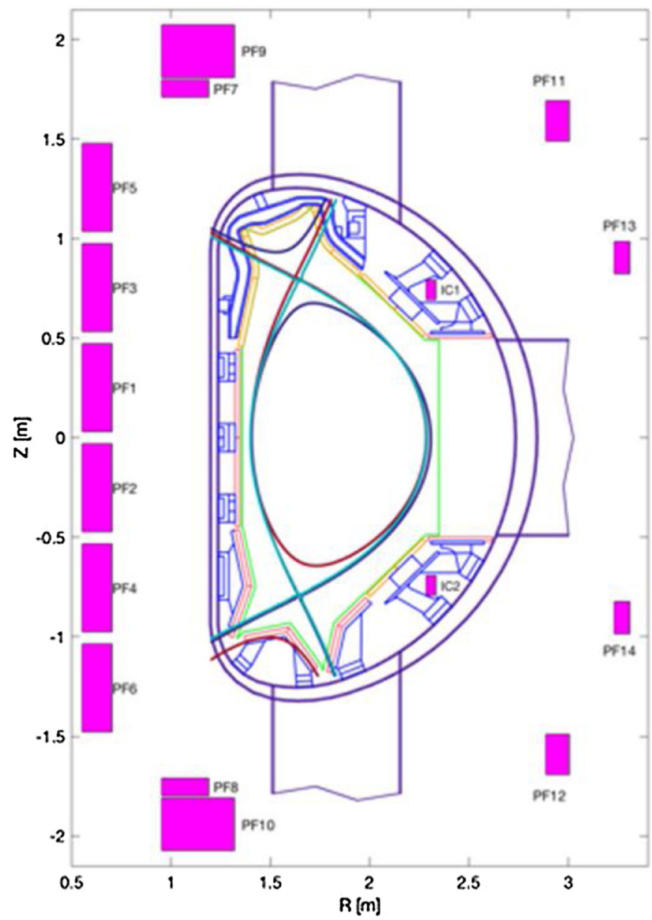

Fig. 1. 2D EAST geometry schematic view, mainly indicating the PF coils and IC coils, the vaccum vessel and first way. The plasma configurations in DN, LSN and USN shown within the device is represented by their last closed flux surface (LCFS).

equilibrium configurations in different stages are designed and optimized by equilibrium code to get the desired I_p, R_p, Z_p, $\varkappa$, ι_i, β_p and plasma boundary coordinates. Then, running discharge simulation code, like TSC [10] or DINA [11], to confirm the equilibrium design results and provide the request PF coil current to PCS. The only problem is the discharge simulation running is a time-consuming process, which is not fast enough to deploy a new configuration discharge. Besides, the equilibrium design of AMD configuration needs to apply more constraints on usual equilibrium code to satisfy the strong requirements on the PF coil currents. In order to obtain the desired AMD configuration with two first-order X points, new constraints for the X points was added as shown in following equation.

$$\frac{\partial\psi}{\partial R} = \frac{\partial\psi}{\partial Z} = 0 \tag{1}$$

$$\frac{\partial\psi^2}{\partial^2 R} = \frac{\partial\psi^2}{\partial^2 Z} = \frac{\partial\psi^2}{\partial R\partial Z} = 0 \tag{2}$$

Two options are provided in F2EQ code, one is setting the gradient of flux and poloidal field to zero with weak weight factor at primary X point only as shown in Eqs. (1) and (2). The second one is setting the gradient of flux to zero at both primary X point and inactive X point. In the equilibrium optimization, the desired plasma boundary coordinates and the position of the X points should be provided as input as shown in Fig. 2. The relation between the PF coils and these target points is described in Eq. (3).

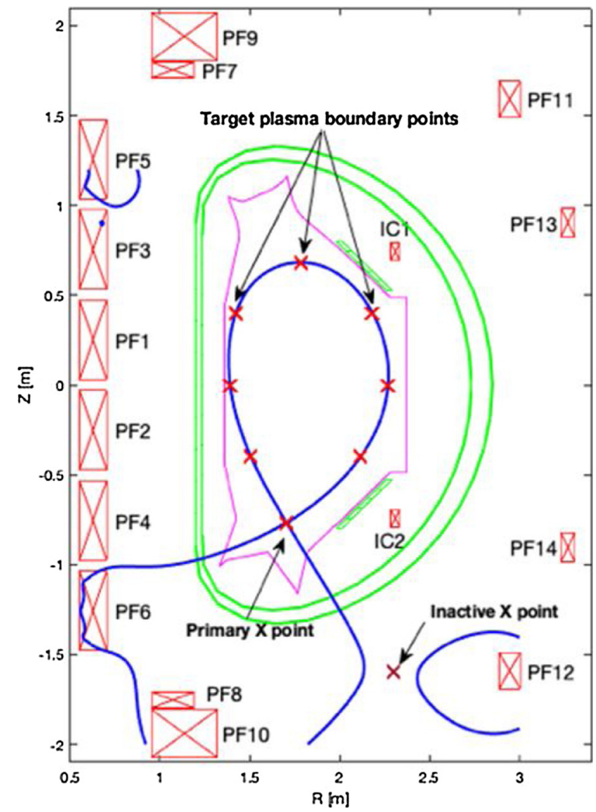

Fig. 2. The desired AMD configuration represented by a contour of LCFS. The target plasma boundary points, primary X point and the inactive X point are shown too.

$$\begin{bmatrix} W_p \cdot M_{pc} \\ w_{x0} \cdot m_{x0c} \\ W_{xB} \cdot G_{xc} \\ W_{PF} \end{bmatrix} \times [I_{PF}] = \begin{bmatrix} \bar{\psi}_{bdry}^{PF} \\ \bar{\psi}_{x0} \\ \bar{B}_x \\ I_{PF}^{con} \end{bmatrix} \tag{3}$$

Here, W_p, W_{xB} and W_{PF} are diagonal matrix of the weight factor for the flux on plasma boundary points, poloidal field on X points and the coils current, w_{x0} is the weight factor for the flux on primary X point. Since the inactive X point may not located in the same flux contour as the primary one, it is no need to set its flux value here. M_{pc}, m_{x0c} and G_{xc} are the green function between PF coils and these target points. I_{PF} is the coil current vector to be solved in this equilibrium. $\bar{\psi}_{bdry}^{PF}$ and $\bar{\psi}_{x0}$ are the flux on boundary points and primary X point produced by PF coils. $\bar{B}_x$ are the poloidal field on X points by PF coils current. I_{PF}^{con} are the applied PF coils current limitation constraints. Since there is plasma contribution too, the plasma current should satisfy the Grad-Shafranov equation.

$$\Delta^*\psi = -\mu_0 R^2 p'(\psi) - \mu_0^2 F(\psi)F'(\psi) \tag{4}$$

The plasma current I_p is an input value to define the plasma flat-top level. And the toroidal current density will be represented as [12]

$$J_\phi = J_0\left[\beta_0\frac{R}{R_c} + (1-\beta_0)\frac{R_c}{R}\right](1-\psi_N^n)m \tag{5}$$

where $\psi_N = (\psi - \psi_a)/(\psi_b - \psi_a)$ is the so-called normalized flux, ψ_b and ψ_a being the flux values at the plasma boundary and at the magnetic axis, respectively, R_c the horizontal coordinate of a characteristic point inside the vacuum vessel, usually as major radius, and β_0, n and m parameters will be setted as input which are related to β_p, ι_i and I_p, J_0 is an automatic regulating factor related to I_p. The total poloidal flux is

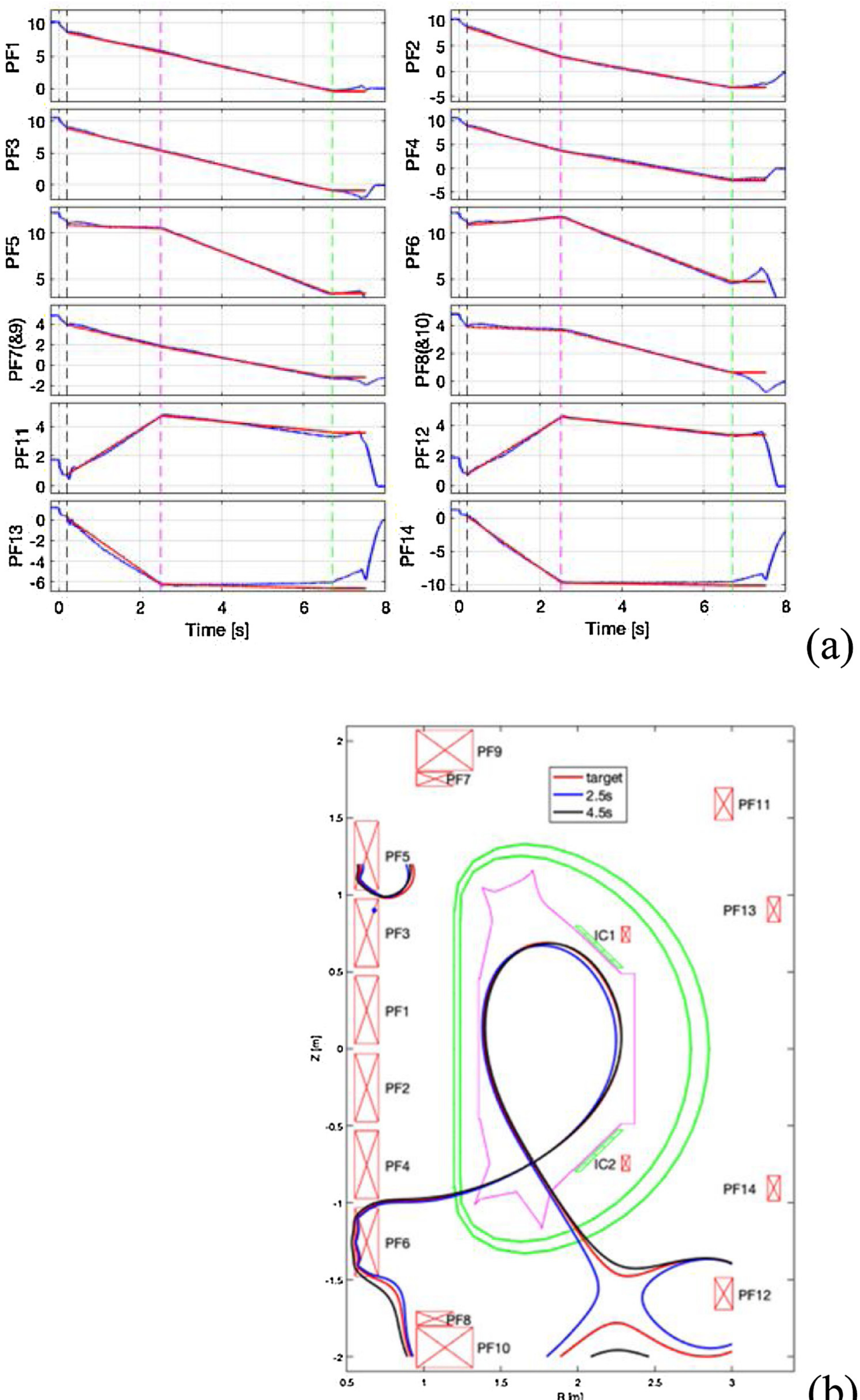

Fig. 3. AMD scenario design results and experiment confirmation. (a) The comparison of the PF coils current waveforms between the real experiment one (Blue) and the designed one; (b) The comparison of the AMD configuration for the target one and the EFIT reconstructed results at 2.5 s and 4.5 s.

$\psi = \psi_p + \psi_c$ with ψ_p produced by the plasma current and ψ_c by the currents in the external PF coils. The equilibrium results will be solved by Picard iterations until the latest two successive flux errors, indicated by the largest change in the calculated grid points, are small enough ($\varepsilon = 10^{-7}$).

$$\left|\frac{\psi^{(k)} - \psi^{(k-1)}}{\psi_b - \psi_a}\right|_{max} \leq \varepsilon \tag{6}$$

In these iterations, the PF coil currents were optimized by least-square solutions. And the plasma boundary was adjusted to fit the given target plasma configuration.

After having the optimized plasma equilibrium with desired AMD configuration, the relevant flux level of this equilibrium and its PF coil currents are obtained. Considering all the PF coils will provide ohmic heating, ohmic current drive and plasma shaping together, the PF coils current can be divided into two components, which are shaping and ohmic part, described as

$$I_{PF} = I_{PF}^{shaping} + I_{PF}^{ohmic} \tag{7}$$

Since the plasma current and target plasma configuration will not change in all the design scenarios, then the shaping coil current component will keep same. Once we have one of the target plasma equilibrium, the PF coils current, in another scenarios, can be obtained by the given ohmic flux consuming, calculated as

$$\begin{aligned} I_{PF1} &= I_{PF1}^{shaping} + I_{PF1}^{ohmic} \\ &= I_{PF0}^{shaping} + I_{PF1}^{ohmic} \\ &= I_{PF0}^{shaping} + I_{PF0}^{ohmic} + \delta\psi \times I_{PF}^{ohmic0} \\ &= I_{PF0} + \delta\psi \times I_{PF}^{ohmic0} \end{aligned} \tag{8}$$

Here, I_{PF0} and I_{PF1} are the PF coils current at different flux level, corresponding to different scenarios. $\delta\psi$ is the flux variation in two different scenarios, and I_{PF}^{ohmic0} is the PF coils current vector corresponding to the normalized ohmic flux distribution. In this new AMD configuration scenarios design, the flux variation in different scenarios was estimated based on the measurement on the flux loops in the routine plasma discharge with same plasma flat-top current. Then all the desired parameters in multiple scenarios needed by PCS system can be provided by this fast scenario design.

In comparison to run the full discharge simulation code, like TSC, the new proposed fast way only needs to design a static equilibrium and then calculate new coils current with given flux levels, the whole process only takes 10–30 seconds, which depends how many iterations in the static equilibrium calculation before reaching a converged result.

3. Experiment confirmation

In the dedicated experiments, the plasma current was purposely chosen to no more than 250kA for device safety. Then the optimized maximum PF coils current can be less than 12.5kA/turn on PF6. In this case, the designed plasma current will reach the flat-top at 1.1 s, and the scenarios for plasma breakdown and ramp-down are inherited from the routine discharge. In order to avoid the voltage limit on coils, it needs long transient before reaching the desired AMD configuration. Then, two AMD scenarios were designed for time slices at 2.5 s and 6.7 s, which leaves 1.4 s for transition to the first desired AMD scenario. The configuration was achieved at 2.5 s with RZIP control till 2.7 s, then switch to ISOFLUX control for more accurate plasma boundary control [13]. Except as the target plasma current centroid, plasma current itself and the feedforward coil currents needed for RZIP control, the ISOFLUX control needs to load the designed plasma shape for LCFS control points calculation (shown in Fig. 2). As shown in Fig. 3(a), The waves in red are designed values, and the waves in blue are the real experiment results. The scenario at 0.2 s for RZIP control is inherited from the routine discharge data without modification. All the intermediating scenarios between these three time slices are obtained by linear interpolation by PCS system. In Fig. 3(b) the target plasma configuration and recontructed plasma separatrix at 2.5 s and 4.5 s by EFIT are shown together. The results show a few differences between the designed one and the real discharge experiment one. It is reasonable, since there was feedback part to control the request parameters, like (R_c, Z_c), I_p, X-points, etc to fit the deigned value by both RZIP and ISOFLUX control algorithm. And the ISOFLUX control can provide stable boundary control to achieve the desired AMD configuration at 4.5 s, then sustained the plasma to ramp-down. In this way, more repeatable discharges in L-mode and H-mode were carried out on EAST [14].

4. Summary

In this paper, a new fast scenario design method for EAST AMD configuration discharge was presented. Code was improved to achieve the AMD configuration, and dedicated experiments confirmed the designed results. Combining the static plasma equilibrium optimization and the flux consuming estimation for PF coils current, this fast scenario design method provides different way for AMD configuration discharges without using time consuming plasma discharge simulation. Based on these design results, stable and repeatable AMD discharges are achieved. New diverted configuration discharge scenarios are built for more EAST physics experiments.

CRediT authorship contribution statement

Z.P. Luo: Conceptualization, Methodology, Software, Writing - original draft. **Y. Huang:** Methodology, Data curation, Investigation, Writing - review & editing. **Q.P. Yuan:** Methodology, Software, Validation. **B.J. Xiao:** Conceptualization, Methodology, Supervision.

Declaration of Competing Interest

The authors declare that they have no known competing financial interests or personal relationships that could have appeared to influence the work reported in this paper.

Acknowledgements

We would like to acknowledge the support and contributions from the rest of the EAST team and collaborators. This work was supported in part by the National MCF Energy R&D Program of China, Grant No. 2018YFE0302105 and National Nature Science Foundation of China, Grant No. 11875291 and 11805236.

Appendix A. Supplementary data

Supplementary material related to this article can be found, in the online version, at doi:https://doi.org/10.1016/j.fusengdes.2020.111816.

References

[1] A. Loarte, et al., Chapter 4: power and particle control, Nucl. Fusion 47 (2007) S203.
[2] T. Eich, et al., Inter-ELM power decay length for JET and ASDEX Upgrade: measurement and comparison with heuristic drift-based model, Phys. Rev. Lett. 107 (2011) 215001.
[3] D.D. Ryutov, Geometrical properties of a “snowflake” divertor, Phys. Plasmas 14 (2007) 064502.
[4] M. Kotschereuther, et al., On heat loading, novel divertors, and fusion reactors, Phys. Plasmas 14 (2007) 72502.
[5] P.M. Valanju, et al., Super-X divertors and high power density fusion devices, Phys. Plasmas 16 (2009) 056110.
[6] Y.X. Wan, et al., Overview progress and future plan of EAST project, Proc. 21th Int. Conf. on Fusion Energy (Chengdu, China) (2006).
[7] B.J. Xiao, et al., EAST plasma control system, Fusion Eng. Des. 83 (2008) 181.
[8] G. Calabrò, B.J. Xiao, S.L. Chen, et al., EAST alternative magnetic configurations: modelling and first experiments, Nucl. Fusion 55 (2015) 083005.
[9] Z. Xing, Study of EAST Discharge Scenario and Plasma Control Based on Free-Boundary Equilibrium, Univ. of Chinese Academy of Sciences, 2016 (In Chinese).
[10] S.C. Jardin, N. Pomphrey, J. De Lucia, Dynamic modeling of transport and positional control of tokamaks, J. Comput. Phys. 66 (1986) 481.
[11] R.R. Khayrutdinov, V.E. Lukash, Studies of plasma equilibrium and transport in a tokamak fusion device with the inverse-variable technique, J. Comput. Phys. 109 (1993) 193.
[12] L.L. Lao, H.St. John, R.D. Stambaugh, et al., Reconstruction of current profile parameters and plasma shapes in tokamaks, Nucl. Fusion 25 (1985) 1611.
[13] Q.P. Yuan, B.J. Xiao, Z.P. Luo, et al., Plasma current, position and shape feedback control on EAST, Nucl. Fusion 53 (2013) 043009.
[14] B.J. Xiao, Z.P. Luo, Q.P. Yuan, et al., Integrated plasma control for long pulse advanced plasma discharges on EAST, Fusion Eng. Des. 128 (2018) 90.